Relativistic Dynamics

Dennis V. Perepelitsa*
MIT Department of Physics
(Dated: December 5, 2006)

The Newtonian and relativistic relationships between the velocity, momentum and energy of an electron traveling at relativistic speeds are compared. Plots of these values are obtained using an electromagnet, velocity selector and solid-state detector. Values of the electron charge and electron rest energy are calculated at $e = 1.44 \pm .02 \times 10^{-19}$ C and $m_e c^2 = 514 \pm 6$ keV, respectively. The possibility of systematic error in the electromagnet is discussed.

1. INTRODUCTION

The familiar Newtonian relationships between the kinetic energy, momentum and velocity of a particle break down as its speed approaches that of light. Instead, a new set of relativistic relations must be brought to bear. By determining these relations at high speeds, we can demonstrate the correctness of relativistic dynamics and calculate the invariant mass and electric charge of the particle under consideration. Though a large amount of energy is typically required to accelerate an object to relativistic speed, such an energy is readily attainable by an electron ejected during beta decay.

2. THEORY

2.1. Theory of the experiment

An electron with charge e moving with velocity $\vec{v}$ inside a magnetic field of strength $\vec{B}$ experiences a force $\frac{e}{c}\vec{v}\times\vec{B}$. If the electron has momentum p and is moving in the plane perpendicular to the direction of the field, it enters a circular trajectory with radius r described by:

$$Ber/c = p \tag{1}$$

We note that the radius of the curvature is dictated entirely by the strength of the field and momentum of the electron. If the electron then enters a region with an electric field $\vec{E}$, it will experience a force in the direction opposite to the field with magnitude eE. If these fields are causing forces to act on the electron in opposite direction, the net force $eE - evB/c$ will cancel for an electron with a certain velocity given by

$$v = c\frac{E}{B} \tag{2}$$

Electrons with a different velocity will be deflected to one side or another, and only when the ratio of the fields is equal to the ratio of the velocity of incoming electrons to the speed of light will the number of electrons that do not deviate significantly from a straight line be highest. This is the principle behind the parallel-plate velocity selector used in the experiment.

2.2. Relativistic dynamics

The Newtonian equations of motion taught in high school are correct to a high degree of accuracy in non-relativistic systems. A particle with velocity v and mass m has momentum $\vec{p} = m\vec{v}$ and kinetic energy given by

$$K = \frac{p^2}{2m} = \frac{1}{2}mv^2 \tag{3}$$

However, these relations must be modified under the postulates of special relativity.[1] A particle with velocity v in an inertial reference frame of reference has momentum γmv in that reference frame, where γ is called the Lorentz factor, and for a particle with velocity v is equal to $\gamma = \frac{1}{\sqrt{1-\frac{v^2}{c^2}}}$. In addition, we define $\beta = \frac{v}{c}$. The inclusion of these terms serves to simply relativistic expressions.

The *total* relativistic energy T of a particle is given by $T^2 = p^2c^2 + m^2c^4 = \gamma mc^2$. The kinetic energy K is the total energy less mc^2 (where mc^2 is known as the particles "invariant rest mass" or "rest energy"), given by

$$K = (\gamma - 1)mc^2 \tag{4}$$

The different expressions for the energy and momentum of a particle will, as we will see, deviate strikingly as v approaches c.

3. EXPERIMENTAL SETUP

Our experimental setup, diagrammed in Figure 1 consisted of a coiled spherical electromagnet, Strontium-90 electron emission source undergoing beta decay, parallel-plate velocity selector, solid-state particle detector and a multi-channel analyzer system in the form of a PC.

*Electronic address: dvp@mit.edu

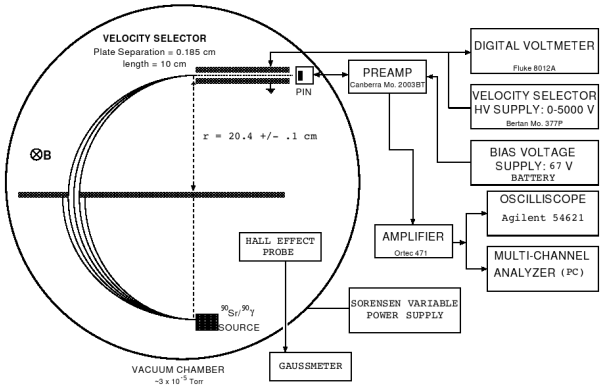

FIG. 1: Diagram of experimental setup, modified from[2]. PIN is the solid-state silicon detector.

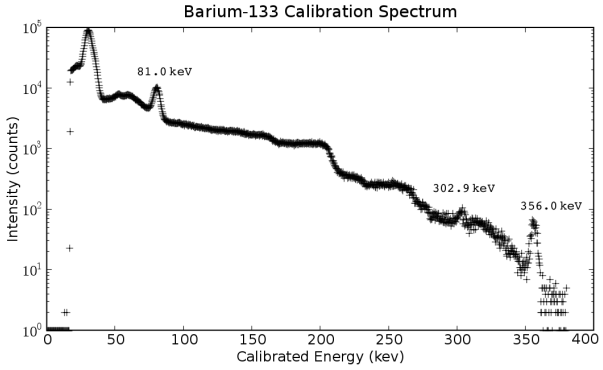

FIG. 2: Energy channel calibration with known radioactive source. The displayed counts were collected over a ten hour period.

The electromagnet had the correct distribution of surface charge to effect a downward-oriented magnetic field. We measured its radius with a meter stick at $r = 20.4 \pm .1$ cm. A variable high-voltage power supply determined the strength of the magnetic field inside the sphere. The magnitude of this field was measured with a gaussmeter, which worked by measuring the Hall Effect across a metal probe inside the sphere. To determine the non-uniformity of the magnetic field inside the electromagnet, we measured the strength of the field in ten different locations inside the sphere. The relative non-uniformity in the field was not more than 1%. Due to limitations in the power supply, $125G$ was the maximum attainable field.

However, this is more than a sufficient magnitude of the magnetic. We were able to observe electrons with $\beta \simeq .8$ with a maximum-magnitude field. The velocity selector consisted of two conducting plates separated by a distance $d = .185$ cm, and the potential difference across them was controlled by a high-voltage source and monitored by a digital voltmeter. Throughout the course of the experiment, this value ranged from 2 to 5 kV.

The silicon solid-state detector, acted on by a $67V$ bias voltage source battery, sent out a positive-voltage pulse with height relative to the magnitude of the energy of the detected particle impacting it. This pulse was caught by the amplifier, and sent to the multi-channel analyzer (MCA) card on a PC, where the intensity of the events colliding with the detector was plotted against energy.

3.1. Methodology

We began each day with a calibration of the gaussmeter using a known-strength magnetic source, and a calibration of the energy spectrum using the energy spectrum of the electron capture of, and de-excitation of the ^{133}Cs daughter of, a ^{133}Ba source. In general, we were able to calibrate the gaussmeter to within 1% of the value of the calibration source. We were careful to keep the metal probe perpendicular to the magnetic field at all times.

For a dozen values of the magnetic field B that ranged from 65 to 125 Gauss, we recorded a two-minute energy spectra for multiple values of V, being careful to take at least six measurement of V in the vicinity of the value V_0 that seemed to cause the maximum number of counts. Our step size was .15kV. Treating the measured intensities as Poisson-distributed, we fit Gaussian profiles to each data set. The uncertainty in the parameter V_0 was on the order of $.5\% - 1\%$ for each value of B, with fits of quality $\chi^2_\nu = .5 - 1.5$. Because of the low error and ideal χ^2_ν, we felt justified in accepting these values of V_0.

We calculated the kinetic energy K of observed events, respectively its uncertainty, by taking the mean, respectively standard deviation, of the median energy channels of the observed intensity/energy distribution. The relative uncertainty in the kinetic energy, when calculated this way, was not more than 1%.

There was significant low-energy noise caused by the presence of the strong magnetic field. We filtered out the first hundred spectrum channels, but the "dead time" during each reading hovered between 10% and 15%. Before each data collection session, we recorded the pressure inside the sphere as displayed on a connected barometer. At no point was it higher than 3.7×10^{-5} torr, which assured a negligibly small rms scattering angle for the electrons in the experiment.

4. DATA ANALYSIS

4.1. Calibration of the energy spectrum

The calibration energy spectrum is pictured in Figure 2. The barium-133 in the calibration source decays into an excited cesium-133 atom by electron capture. The branching ratios and energies of the initial excited and all the intermediate excited states of cesium are well-known [3], and thus the relative intensities of observed photopeaks is a clue as to their identity.

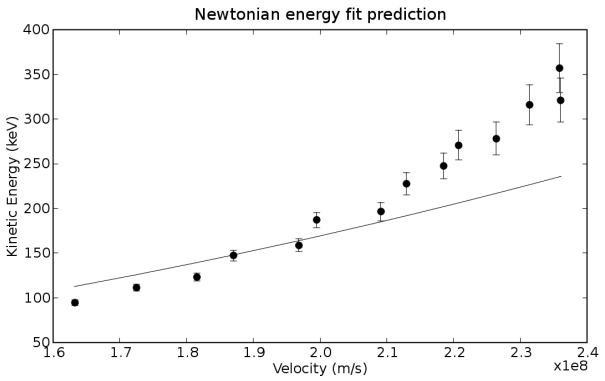

FIG. 3: Attempted fit to the Newtonian energy-velocity relation, with adverse results.

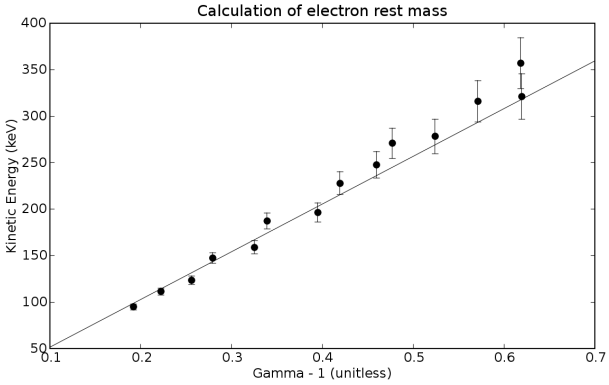

FIG. 4: Linear relation between kinetic energy and $\gamma - 1$.

However, the efficiency of the photoelectric effect in silicon is significantly less than that of the Compton effect for photons with energies higher than $100 - 200$ keV [2]. Thus, the Compton edges, caused by a scattering (instead of absorption) of photons by the detector, are the most prominent feature, although several photopeaks are individually detectable. We identified three of the most prominent cesium-133 gamma ray energies, 81.0 keV, 302.9 keV and 356.0 keV with a single channel each, and constructed a calibration for the rest of the channels. We observed a slight positive zero offset of approximately 3 keV, which we corrected for.

4.2. Relativistic and classical plots

Consider a particular combination of fields $E\ (= V_0/d)$ and B. Particles arriving between the parallel plates of the velocity selector had to have a specific momentum given by (1), and a specific velocity $v = \frac{E}{B}c$ to not deviate once inside the plates. Thus, the value of V_0 that maximizes the number of electrons hitting the solid-state detector is the value of the voltage at which the net force from the magnetic and electric fields cancel. At this value, the particle's velocity is given by rearranging 2 to find $v = V_0 c/Bd$. The spread of kinetic energy is displayed on the MCA. Thus, for a given pair of matched values B, V_0, we are able to either directly measure or calculate the velocity, momentum and energy of observed electron events colliding with the detector.

Having obtained data points (v, p, K), we set out to determine how effective the Newtonian equations are. An attempted non-linear fit of the form $K(v) = \frac{1}{2}m_e v^2$ is shown in Figure 3. The value of electron rest energy is calculated at $m_e c^2 = 763 \pm 9$ keV with a reduced-chi-squared of $\chi^2_\nu = 11.73$, which corresponds to a likelihood infinitesimally close to zero. These results demonstrate the ineffectiveness of the Newtonian equations of motion at relativistic speeds.

Thus, we turn to the predictions of relativistic dynamics to explain our data.

4.3. Determination of $m_e c^2$

We plot K against $\gamma - 1$ in Figure 4. Before we can attempt a linear fit, we must express the error in the value on the ordinate in terms of the basic uncertainties in V_0, B and K.

The uncertainty in the independent parameter is not negligible compared to that of the independent parameter and following Bevington [4], we calculate the contribution $\sigma_{KI} = \frac{d(K)}{d(\gamma-1)}\sigma_{\gamma-1}$ from the uncertainty of $\gamma - 1$ to K, and add it in quadrature to the direct contribution σ_{KD}. The error in γ, in turn, is related to the error in $\beta = \frac{V_0}{Bd}$, which is in turn related to the error in those two quantities:

$$\sigma_\gamma^2 = \frac{\beta^2}{(1-\beta^2)^3}\sigma_\beta^2 \tag{5}$$

$$\sigma_\beta^2 = \frac{1}{B^2 d^2}\sigma_{V_0}^2 + \frac{V_0^2}{d^2}\sigma_B^2 \tag{6}$$

Having calculated the uncertainty in K, we obtain the linear fit shown in Figure 4 and determine the slope to be $mc^2 = 514 \pm 6$keV, with a reduced-chi-squared of $\chi^2_\nu = 1.32$.

4.4. Determination of $e/m_e c^2$

Equating the relativistic equation for momentum with (1), algebraic manipulation obtains $\gamma\beta = B\frac{er}{mc^2}$. Let $S = \frac{er}{mc^2}$. We intend to manipulate this relation into a form convenient for error analysis and fitting. The term on the left can be expressed in terms of $\beta = \frac{V_0}{Bd}$. Significant algebraic manipulation yields

$$V_0 = \frac{B^2 S d}{\sqrt{1 + B^2 S^2}} \tag{7}$$

We plot V_0 against B in Figure 5. As above, the error in the independent variable contributes significantly to the error in the dependent variable. Specifically, the

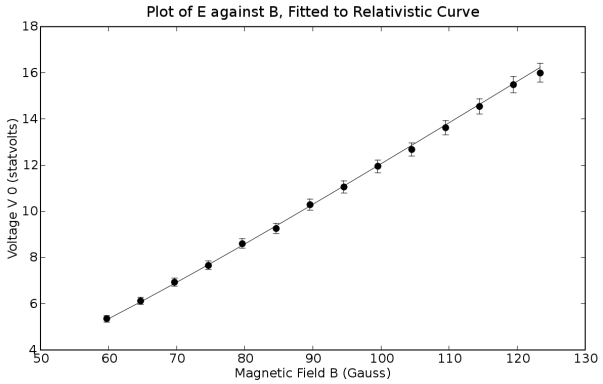

FIG. 5: Restatement of momentum-velocity relation in terms of E and B, and fitted line.

uncertainty σ_{V_0} has a direct contribution σ_{VD} and a contribution from the independent variable $\sigma_{VI} = \left(\frac{dV_0}{dB}\right)\sigma_B$ added in quadrature. For every pair of values (V_0, B), we determine this derivative computationally to obtain an appropriate error term.

Having calculated the uncertainty in V_0 from all sources, we obtain the non-linear fit shown in Figure 5 and determine the single free parameter to be $S = \left(\frac{er}{mc^2}\right) = .0107 \pm .0001 \ \frac{\text{stat-coulombs-cm}}{\text{erg}}$, with a reduced-chi-squared of $\chi^2_\nu = 0.13$. Dividing out r, and adding its error to the error in the slope in quadrature, we obtain the value $e/m_e c^2 = 5.25 \pm .06 \ \times \ 10^{-4} \ \frac{\text{stat-coulombs}}{\text{erg}}$.

The low reduced-chi-squared in the fit hints at an overestimation of the error. In particular, we may be incorrectly considering the "non-uniformity" in the magnetic field to be random error, where it could be considered systematic error. Consider that to enter the velocity detector, an electron must along a relatively distinctive path, and while B may vary across the electromagnet, perhaps it does not change that much along the path taken by the particle. If this were the case, we would want to consider the possibility that we are under- or over-measuring the magnitude of the magnetic field. On the one hand, this might lead to a better adjusted value of $\frac{e}{m_e c^2}$, while shrinking the error bars in each measurement of B and raising the χ^2_ν of a fit closer to 1. On the other hand, this would have an adverse effect on our value of $m_e c^2$.

Since we are relatively confident from our calculation of the electron rest energy that no such systematic error exists, we decide against pursuing this avenue.

4.5. Determination of e

The electron charge is now a product of two measured values, $e = \left(\frac{e}{mc^2}\right)(mc^2)$. We convert the former of these to SI units: $\frac{e}{mc^2} = 5.25 \times 10^{-4} \frac{\text{stat-coulomb}}{\text{erg}} = 2.81 \times 10^{-22}\text{C/keV}$. Taking their product, and adding the relative uncertainties in quadrature as dictated by [4], we obtain

$$e = (2.81 \times 10^{-22}) \cdot (514) = 1.44 \times 10^{-19} \text{ C} \tag{8}$$

$$\sigma_e = e\sqrt{\left(\frac{.06}{5.25}\right)^2 + \left(\frac{6}{514}\right)^2} \tag{9}$$

Our calculated value of the electron charge is $e = 1.44 \pm .02 \times 10^{-19}\text{C}$.

5. CONCLUSIONS

Our calculated value of the electron rest energy $m_e c^2 = 514 \pm 6$ keV is in excellent agreement with the literature value of $m_e c^2 = 511$ keV. Additionally, the strength of the fit ($\chi^2_\nu = 1.32$) of K against $\gamma - 1$ upholds the theoretical linear relation between these values as postulated under relativistic dynamics.

Our calculated value of the ratio of the electron charge to the electron rest energy $\frac{e}{mc^2} = 5.25 \pm .06 \times 10^{-4} \frac{\text{stat-coulombs}}{\text{erg}}$, however, is more suspect. It is more than ten standard deviations away from the literature value of $\frac{e}{mc^2} = 5.87 \times 10^{-4} \frac{\text{stat-coulombs}}{\text{erg}}$. Additionally, the fit of the line is poor: $\chi^2_\nu = .13$. The latter result hints at several possibilities of the underlying reason for this discrepancy, which we have discussed above.

We have no simple explanation for the large discrepancy in this result. The fact that the electron rest energy has a value close to the literature seems to be inconsistent with that of the electron charge. We hope to repeat this part of experiment and derive a better result, or, at least, come to an understanding of why this one is so shoddy.

[1] A.P.French, *Special Relativity* (MIT, 1968).
[2] J. L. Staff, *Relativistic dynamics lab guide* (2004), jLab E-Library, URL `http://web.mit.edu/8.13/www/JLExperiments/JLExp09.pdf`.
[3] *Table of nuclides - korea atomic energy research institute*, URL `http://atom.kaeri.re.kr/`.
[4] P. Bevington and D. Robinson, *Data Reduction and Error Analysis for the Physical Sciences* (McGraw-Hill, 2003).

Acknowledgments

DVP gratefully acknowledges Brian Pepper's equal partnership, as well as the guidance and advise of Professor Chuang, Dr. Sewell and Scott Sanders.